Heart Rate Variability-Based Obstructive Sleep Apnea Events Classification Using Microwave Doppler Radar

Syed Doha Uddin, *Student Member, IEEE*, Md. Shafkat Hossain, *Student Member, IEEE*, Shekh M. M. Islam, *Senior Member, IEEE*, and Victor Lubecke

***Abstract*—Obstructive Sleep Apnea (OSA) is the most common type of sleep disorder that consists of multiple episodes of partial or complete closure (apnea, hypopnea) of the upper airway during sleep and underdiagnosed problems as there is no reliable portable in-home sleep monitoring system. Doppler radar system is gaining attention as an in-home sleep monitoring system due to its non-contact and unobtrusive form of measurement. Prior research on Radar-based sleep monitoring systems mostly focused on distinguishing apnea and normal breathing patterns using radar-reflected signal amplitude that can't distinguish accurately apnea and hypopnea events. Apnea and hypopnea events were distinguished using effective radar cross-section (ERCS) for short-scale study and ERCS changes with sleeping postures and so on. In this work, we proposed a heart rate variability-based robust feature extraction technique to distinguish different sleep disorder events such as apnea, hypopnea, and normal breathing. HRV-based feature extraction technique was employed on ten consented OSA participants' clinical studies to find a distinguishable feature known as the power of the low-frequency band (0.04-0.15 Hz) and high-frequency band (HF) (0.15-0.4 Hz). The extracted hyper-feature (HF and LF) was then integrated with the traditional Machine learning classifiers (ML) including k-nearest neighbors (KNN), support vector machine (SVM), and random forest. SVM outperformed other classifiers with an accuracy of 97% for distinguishing different OSA events that also supersedes other reported results (ERCS). The proposed method has several potential applications including in-home sleep monitoring, OSA severity detection, respiratory disorder detection, and so on.**

***Index Terms*—Doppler radar, heart-rate variability (HRV), machine learning (ML), sleep disorder, in-home sleep monitoring.**

Manuscript received 13 June 2023; revised 15 August 2023; accepted 14 September 2023. Date of publication 27 September 2023; date of current version 22 November 2023. This work was supported by University Grants Commission (UGC) Research Grant, University of Dhaka 2021-2022 (Project ID: 06) and in part by U.S. National Science Foundation under Grant IIS191573. *(Syed Doha Uddin and Md. Shafkat Hossain contributed equally to this work.) (Corresponding Author: Shekh M. M. Islam.)*

This work involved human subjects or animals in its research. Approval of all ethical and experimental procedures and protocols were granted by the ethical review committee of Faculty of Biological Sciences, University of Dhaka, Dhaka-1000, Bangladesh under project no 18, and performed in line with the ethical clearance of research proposal involving human participants and the animal experimentation of ethical review committee (AEERC).

Syed Doha Uddin, Md. Shafkat Hossain, and Shekh M. M. Islam are with the Department of Electrical and Electronic Engineering, University of Dhaka, Dhaka 1000, Bangladesh (e-mail: syeddoha-2017414894@eee.du.ac.bd; md-shafkat-2017914880@eee.du.ac.bd; shekh@hawaii.edu).

Victor Lubecke is with the Department of Electrical and Computer Engineering, University of Hawaii at Manoa, Honolulu, HI 96822 USA (e-mail: lubecke@hawaii.edu).

Digital Object Identifier 10.1109/JERM.2023.3317304

I. Introduction

OBSTRUCTIVE sleep apnea (OSA) is the most common type of breathing difficulty during sleep and it is also among the most frequently underdiagnosed health problems [1]. Studies show that OSA patients have a high risk of diabetes, hypertension, atrial fibrillation, coronary artery disease, and so on [2], [3], [4]. OSA is characterized by repetitive airflow reduction (hypopnea) or cessation (apnea) due to the complete or partial obstruction of the upper airway during sleep [5]. According to the American Academy of Sleep Medicine (AASM), apnea episodes consist of complete cessation of breathing during sleep for at least 10 seconds and hypopnea occurs when the airway is partially collapsed resulting in shallow breathing during sleep [5]. Determining the occurrence of apnea and hypopnea episodes during sleep plays an important role in the diagnosis of the presence and severity of sleep apnea [6]. Although sleep apneas are relatively easy to detect by analyzing breathing frequency, sleep hypopnea, which is defined as a 30% drop in airflow lasting 10 seconds accompanied by either arousal or a 3% drop in peripheral capillary oxygen saturation (SpO2) can not be detected by frequency analysis [6]. To date, Polysomnography (PSG) is the gold standard technique for diagnosing OSA [7]. Although PSG requires a dedicated sleep laboratory where trained technicians need to be involved in monitoring patients, and at the same time, patients need to wear different sensors on the body surface such as the electrocardiogram (ECG), electroencephalogram (EEG) and so on [8]. Patients feel uncomfortable during PSG tests especially if it requires a whole night study and it can also hamper the sleep behavior of patients [9]. Additionally, PSG is an expensive medical testing procedure where a dedicated sleep laboratory is required with a trained sleep technician [10]. Therefore, there are growing need and interest in developing portable, non-contact, and unobtrusive sensing methods for detecting OSA and its associated breathing pattern events (normal, apnea, and hypopnea) so that patients can take this test in the home environment without attaching any sensor to the body surface [10], [11].

People also attempted to use video cameras for unobtrusive sleep apnea detection [12]. Radar technology seems more promising than cameras as being monitored by a camera always brings privacy concerns [13]. Radar analyzes the phase modulation of the reflected signal induced by the minute movement of the chest surface owing to cardio-respiratory activities, making

2469-7249 © 2023 IEEE. Personal use is permitted, but republication/redistribution requires IEEE permission.
See https://www.ieee.org/publications/rights/index.html for more information.

Authorized licensed use limited to: UNIV OF HAWAII LIBRARY. Downloaded on May 05,2025 at 21:27:57 UTC from IEEE Xplore. Restrictions apply.

it a promising non-contact vital signs monitoring tool that is privacy-invasive [14]. Prior research demonstrated the feasibility of using radar technology for diagnosing OSA using various methods such as manual reading [15], amplitude thresholding [16], and classical machine learning with handcrafted features [17], [18]. All of the attempts described here mostly focused on recognizing apnea events from the normal breathing pattern and shows promising results. However, for detecting the severity of OSA, distinguishing between apnea, and hypopnea from normal breathing patterns is very critical [19]. To the best of our knowledge, two research works have also attempted to distinguish between apnea, hypopnea, and normal breathing patterns using microwave Doppler radar [20], [21]. In an attempt [20], effective radar cross-section (ERCS) has been used to distinguish between different apnea events with an accuracy of 96.7%. However, the study was performed on a short scale with just five participants in a clinical study and ERCS is dependent on the transmitted signal frequency, and it changes with the sleeping postures or torso orientation [22]. Additionally, the reported result in [20] used was for five patients with 20 minutes of data for each patient. In this work, we reanalyzed the ERCS method for a large-scale ten-patient dataset consisting of 394 minutes (6 hours) of each patient and the accuracy degrades to 78.2%. Moreover, The errors and difficulties in the center estimation and imbalance compensation make the use of the arc radius feature (ERCS) less accurate. Therefore, the method is not robust and cannot be implemented in a realistic setting as people may sleep in different postures. In another attempt [21], 60-GHz frequency-modulated continuous wave (FMCW) radar was utilized where radar data was segmented for 30 seconds, and segment-wise z-score normalization was performed based on the mean and standard deviation of the signal for the automated detection of apnea, and hypopnea events for OSA diagnosis with an accuracy of 73.6% [21].

In [16], the amplitude threshold algorithm can isolate paradoxical breathing (apnea or hypopnea events combined) and normal breathing with an accuracy of 92% but can isolate apnea, hypopnea, and normal breathing individual events with an accuracy of 73.6% only. Additionally, this algorithm's decision criteria based on the amplitude of the signal for isolating apnea and hypopnea did not work accurately for 2.4 GHz and 24 GHz radar systems individually, which creates ambiguity in isolating these two events (apnea and hypopnea). Moreover, signal amplitude may vary based on the propagation characteristics of the surroundings. Therefore, a robust feature extraction technique is required for automated apnea, and hypopnea events classification using microwave Doppler radar.

This article proposes a new and robust heart rate variability (HRV)-based feature extraction technique and also explores the feasibility of this technique to recognize different respiratory disorder events from ten OSA patients' clinical study data with an accuracy of 97% that supersedes all the reported literature results. The core contribution of this work is to find the distinguishable HRV features for the reliable classification of different OSA events. HRV is a method that represents beat-to-beat oscillations and is considered a measure of neuro-cardiac function that also reflects the automatic nervous system [23]. It has been found in the literature that the magnitude of variability of the HRV is

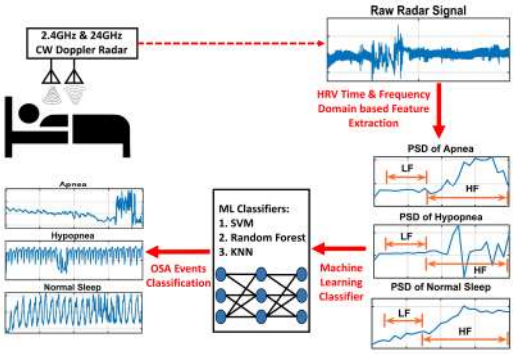

Fig. 1. Block diagram of the proposed system. The proposed system consists of CW radar and then using signal processing approaches HRV features were extracted. From the distinguishable HRV features, OSA events can be classified by integrating ML classifiers.

associated with the severity of OSA [24], [25]. Thus, the HRV feature extraction method has been chosen for our work, which shows a good correlation with OSA events and also supersedes the accuracy. The core contribution of this work is as follows:

1) A new and robust HRV-based feature extraction technique has been proposed and its feasibility has been tested for clinical study OSA datasets and the accuracy of the system supersedes other reported results.
2) We have found hyper-features known as the power of the low-frequency band (LF) (0.04-0.15 Hz) and high-frequency band (HF) (0.15-0.4 Hz) that show significant variations for different respiratory patterns from the clinical study of OSA patients' data and showed superior performance
3) Traditional machine learning (ML) approaches have been integrated with the extracted feature set.

II. Material and Methods

The proposed system for OSA events classification includes capturing physiological signals using continuous wave (CW) Radar, extracting the HRV features from it, and then classifying the OSA events using distinct features integrated with machine learning classifiers. The dataset used in this work is from the clinical study of ten OSA patients using 2.4 GHz and 24 GHz radar that was reported in a prior research attempt [16]. We also extracted HRV time and frequency domain features from the radar-captured signals and then tried to find some distinguishable features to recognize different OSA events by integrating ML classifiers. For the verification of the different OSA events, we also used sandman data and compared our result with the standard sandman measurement which is used as the gold standard method [16]. The schematic diagram of the proposed system is shown in Fig. 1. The rest of the subsection discusses the radar system, the procedure of sleep study, the theory of microwave Doppler radar for the OSA study, and HRV feature extraction validation

A. Radar System

In this work, we used a clinical dataset from prior reported results [16] that used a 2.4 GHz and 24 GHz combined radar system shown in Fig. 2. This system was used to acquire data

Authorized licensed use limited to: UNIV OF HAWAII LIBRARY. Downloaded on May 05,2025 at 21:27:57 UTC from IEEE Xplore. Restrictions apply.

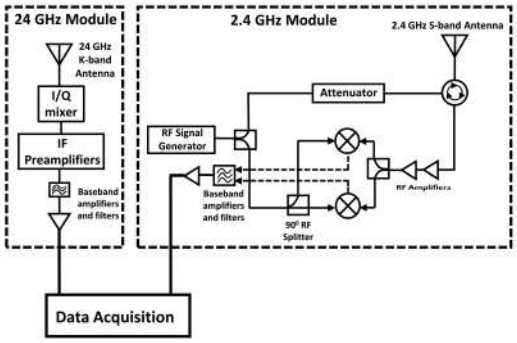

Fig. 2. Radar module combination of 2.4 GHz and 24 GHz used for OSA clinical study. Taken from [16].

from the OSA patients, and clinical study data was reported in prior research efforts [16]. The 24 GHz radar was a commercial K-MC1 module from an RF beam Microwave (Rfbeam Microwave GmbH, Gallen, Switzerland) containing a 24 GHz K-band antenna with an RF LNA and two IF preamplifiers [26]. The 2.4 GHz radar was assembled using coaxial components [16]. Digitized data were acquired from both the outputs of the 24 GHz and 2.4 GHz radar using the National Instrument data acquisition module (NI-USB 6259, National Instruments, Austin, TX, USA) and used for analysis later on [16]. The transceiver antenna of the radars was placed above the chest of a patient in a supine position so that the chest and abdomen movement could be perpendicular to the plane of the antenna. There was an approximate distance of one meter between the antenna and the patient's chest so that the patient's movement wasn't hampered during sleep [16].

B. Sleep Study Dataset

The OSA patients' data was acquired from a previous study which was approved by the Institutional Review Board of the University of Hawaii at Manoa the study was performed at the Queen's Medical Center, Honolulu, HI, USA [16]. Ten known OSA patients volunteered to participate in the study at a certified sleep study center (Queen's Medical Center, Honolulu, HI, USA) [16]. All the participants wore loose-fitting two-piece sleepwear and the efficacy of Doppler radar remote respiration sensing through clothing and other obstacles has been demonstrated in prior studies [27], [28], [29]. Prior written consent regarding the study was taken from the participants and it was prohibited for them to use the Continuous Positive Airway Pressure (CPAP) machine while the study was underway. The radar system was incorporated with a PSG system (GOLD standard) from Embla called the Sandman System [16]. A practicing sleep technician scored the PSG data after every test. Apnea and Hypopnea events were marked with timestamps for each recorded data and the same time indexes from the radar data were separated to extract HRV features from those time-segmented data.

C. Theory of Respiratory Pattern Acquisition Using Radar

The quadrature baseband data obtained from the radar system shown in Fig. 2 has been used to detect the apnea events from a sleep study. The Doppler radars in this system have two receiver output channels, one is in-phase (I) and another one is quadrature-phase (Q). The advantage of using a quadrature receiver is that it fixes the null point problem the single-channel radars have [28]. The two quadrature outputs can be mathematically expressed as [29]:

$$B_I(t) = \text{Asin}\left(\theta + \frac{4\pi x(t)}{\lambda} + \Delta\varphi(t)\right) \tag{1}$$

$$B_Q(t) = \text{Acos}\left(\theta + \frac{4\pi x(t)}{\lambda} + \Delta\varphi(t)\right) \tag{2}$$

Where, $B_I(t)$ is the in-phase channel signal, $B_Q(t)$ is the quadrature-phase channel signal, $x(t)$ is the chest displacement, A is the signal amplitude, λ is the wavelength of the transmitted signal, $\Delta\emptyset(t)$ is the residual phase noise and θ is the constant phase shift [29]. The tiny chest movements during breathing can be found as a phase shift in the reflected radar signal [29]. I/Q imbalance of the quadrature radar data was corrected by the Gram-Schmidt method and DC offset calibration was performed by removing the DC offset terms in I/Q channels [16]. Arctangent demodulation technique has been used to extract the maximum chest displacement information from the quadrature radar shown in (3), [29].

$$\begin{aligned}\varphi(t) &= \text{unwrap}\left(\arctan\left(\frac{B_Q(t)}{B_I(t)}\right)\right)\\ &= \text{unwrap}\left(\arctan\left(\frac{\cos(\theta + p(t))}{\sin(\theta + p(t))}\right)\right) = \theta + p(t))\end{aligned} \tag{3}$$

We also used the Matlab unwrap function to mitigate the phase wrapping issue. This function unwraps the radian phase angles in a vector $\phi(t)$. Whenever the jump between consecutive angles is greater than or equal to π radians, unwrap shifts the angles by adding multiples of $\pm 2\pi$ until the jump is less than π. Here, $p(t) = 4\pi x(t)/\lambda$. The chest displacement information can be approximated from (4) as follows:

$$\varphi(t) \approx \frac{4\pi x(t)}{\lambda} \tag{4}$$

where $\varphi(t)$ is the phase of the signal and $x(t)$ is the chest displacement. Prior research has demonstrated that there are amplitude and arc of the radius changes in the radar signal during apnea and hypopnea events [16], [20].

D. HRV Feature Extraction Validation

We have taken 60-second windows for HRV parameter calculation. The extracted time domain and frequency domain HRV metrics have been enlisted in Table I shown below [30].

1) *Heart Rate:* Generally, we can find heart rate (HR) from the number of cardiac cycles within a certain amount of time [30]. Fast Fourier Transform (FFT) is another signal-processing approach to finding the HR on the collected respiration segment. For heart rate waveform extraction we used a bandpass filter with a cut-off frequency of 0.8–2 Hz.
2) *Standard Deviation of Successive Differences (SDSD) of RR intervals:* For instance, if the recorded data has N

Authorized licensed use limited to: UNIV OF HAWAII LIBRARY. Downloaded on May 05,2025 at 21:27:57 UTC from IEEE Xplore. Restrictions apply.

TABLE I
EXTRACTED HRV METRICS

Categories	Indexes	Features
Typical Features	1	Heart Rate
	2	Standard Deviation of Successive Differences of RR intervals (SDSD)
	3	Standard deviation of IBI's (SDNN)
	4	Root Mean Square of Successive Differences of IBI's (RMSSD)
	5	NN50 (NN intervals that differ more than 50 ms)
	6	Percentage of power in Low frequency Band (pLF)
	7	Percentage of High Frequency Band Power (pHF)
	8	LF/HF ratio
	9	Threshold Voltage for R peak Detection (Vth)
Hyper-Features	1	Power of Low Frequency Band (LF)
	2	Power of High Frequency Band (HF)

heart cycles and the peaks can be denoted as R_{xi}, then the set of peaks can be expressed as:

$$R_{ex} = [R_{x1}, R_{x2}, R_{x3}, R_{x4}, \ldots, R_{xN}] \quad (5)$$

The time of occurrence of each peak is denoted by t_{px_i}. The time interval between two R peaks is denoted by Interbeat Interval (IBI). It can be expressed as:

$$T_{IBIi} = t_{px_{i+}} - t_{px_i} \quad (6)$$

The successive differences of the interbeat interval are represented by the below equation

$$T_{SDi} = T_{IBIi+1} - T_{IBIi} \quad (7)$$

After acquiring a set of successive differences of R-R peaks in a time segment, we can find the standard deviation of that is known as SDSD and it can be represented by the below equation [30]:

$$SDSD = \sqrt{\sum\nolimits_{i=1}^{N} \frac{1}{N}(T_{SDi+1} - T_{SDi})^2} \quad (8)$$

Here, N is the number of beats in the segmented window

3) *Standard deviation of IBI's (SDNN):* For measuring the standard deviation of sinus beats of a segmented window, we need the time interval between two R peaks. R-R interval can be extracted using (6). After finding (IBI) within a specified window size, SDNN is calculated by the below equation [30]:

$$SDNN = \sqrt{\sum\nolimits_{i=1}^{N} \frac{1}{N}(T_{IBIi+1} - T_{IBIi})^2} \quad (9)$$

Here, T_{IBIi} is the interbeat interval of two R peaks.

4) *Root Mean Square of Successive Differences of IBI's (RMSSD):* We obtain the root mean square of successive differences between normal heartbeats by calculating successive time differences from (7) for a time window. Then we find the root mean square of the values of all successive differences in that segment from the following equation [30]:

$$RMSSD = \sqrt{\frac{1}{N}\sum\nolimits_{i=1}^{N} T_{SDi}^2} \quad (10)$$

5) *NN50:* NN50 is calculated by measuring the number of adjacent interbeat intervals, which have a difference of at least 50ms. It is easily acquired from the difference between IBI's.
6) *Power of Low-Frequency Band (LF):* After converting the time domain signal into the frequency domain signal, we calculated the power spectral density by taking the square of the absolute value of the normalized magnitude of the FFT. The Low-Frequency (LF) band power is measured by taking the summation of powers for frequency components within the region of 0.04 to 0.15 Hz.
7) *Power of High-Frequency Band (HF):* The High-Frequency (HF) band ranges from 0.15 Hz to 0.40 Hz. Similar to LF band power, HF is measured by taking a summation of powers in the HF region. Fig. 6 shows the HF in the PSDs of different respiratory events.
8) *Percentage of power in Low-frequency Band (pLF):* We can compute the overall percentage of LF band power in the total power of the signal consisting of HF band power and LF band power using (11).

$$pLF = \frac{LF}{LF + HF} \times 100 \quad (11)$$

9) *Percentage of High-Frequency Band Power (pHF):* We can compute the overall percentage of HF band power in the total power of the signal consisting of LF band power and HF band power using (12).

$$\mathrm{pLF} = \frac{\mathrm{HF}}{\mathrm{LF} + \mathrm{HF}} \times 100 \quad (12)$$

10) *LF/HF ratio:* LF/HF ratio can be computed by taking the ratio of LF band power and HF band power in a time window.
11) *Threshold Voltage for R Peak Detection (Vth):* The threshold voltage (Vth) has been used to detect R peaks in a heart signal [30]. The zero-crossing method is a common method for detecting peaks, but it can overestimate the number of peaks due to noise and harmonics of the respiratory signal in the same frequency band [31], [32]. To mitigate this problem, the threshold voltage is used as a baseline for detecting peaks instead of using a zero-voltage baseline. The threshold voltage is calculated as the average root mean square voltage of all the peaks detected using the zero-crossing method, divided by two. This helps to reduce the number of false positives and improve the accuracy of peak detection in the heart signal. In (13), we can see that Vth is the half of average root mean square voltage of all peaks in the zero-crossing method.

$$\mathrm{V_{th}} = \frac{1}{2\mathrm{n}} \sum_{\mathrm{i}=1}^{\mathrm{n}} \frac{|\mathrm{V_{mag}}\,(\mathrm{i})|}{\sqrt{2}} \quad (13)$$

Authorized licensed use limited to: UNIV OF HAWAII LIBRARY. Downloaded on May 05,2025 at 21:27:57 UTC from IEEE Xplore. Restrictions apply.

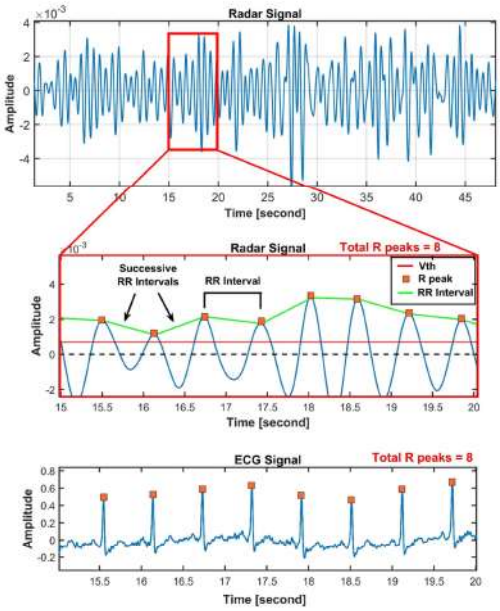

Fig. 3. Radar heart signal in the time domain with a duration of 5 seconds showing the R peaks, R-R intervals & threshold voltage (Vth), and its comparison with the ECG signal from the same subject. Here, Vth is indicated by a red line, and the RR intervals (green line) are measured using the distance between two R peaks (orange square). The R peaks of the radar match with that of the ECG acquired signal. The HRV time domain metrics SDSD, SDNN, RMSSD, and NN50 can be extracted using the R peaks and R-R intervals of the radar signal.

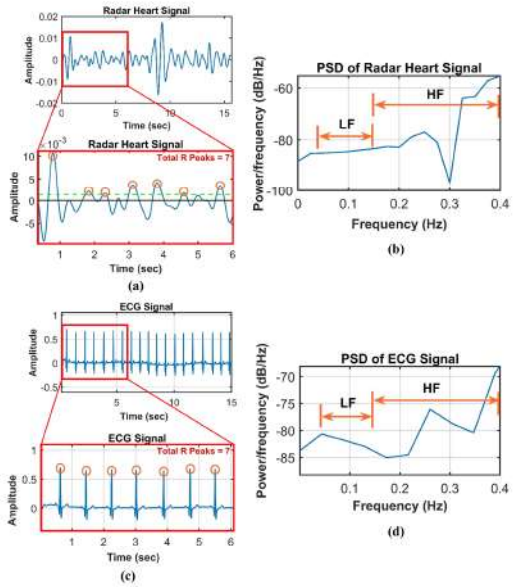

Fig. 4. Heart signals recorded from a single subject using radar and ECG (a, and c) and their respective PSDs (b, and d). The LF and HF power from the PSD of radar heart signal correlates with that of the ECG signal, where the LF power resides between −80 dB/Hz to −85 dB/Hz and the HF power between −60 dB/Hz to −80 dB/Hz. The number of R peaks of the radar matches accurately with the ECG signal as well.

In the above equation, N is the number of peaks from the zero crossing method in a time segment. Fig. 3 illustrates the threshold voltage in the heart signal. For initial validation purposes, we collected data from five normal healthy participants using 24-GHz CW radar. The radar that was used in this case was a commercial K-LC1a module from RF beam Microwave (Rfbeam Microwave GmbH, Gallen, Switzerland). It is an 8-patch module with a 24 GHz K-band antenna [26]. It has a beam aperture of 80°/34° [26]. With the approval of the Ethical Review Committee of the Faculty of Biological Sciences, University of Dhaka, we collected data from five human subjects using the K-LC1a radar module all within the age of 21–25. For comparison purposes, we also used the ECG reference BSL MP46 from BIOPAC Systems Inc., which is a 2-channel ECG data acquisition device. Using the RR intervals from both the radar and ECG data, different HRV time and frequency domain metrics were extracted and their accuracy with the ECG-extracted HRV parameter was calculated. The efficacy analysis of HRV parameter extraction using Radar and ECG has been reported by our group recently [33]. Our analysis indicated that the accuracy of the proposed HRV extraction was always above 93% both for the time domain and frequency domain parameters [33]. Fig. 4 illustrates the comparison between the PSDs of the radar heart signal and the reference ECG signal of a single subject. The LF and HF power of the radar closely matches the ECG. The LF power of both the radar and the ECG ranges from −80 dB/Hz to −85 dB/Hz. The HF power of the radar, although goes 10 dB/Hz higher than the reference ECG but the power decline at 0.3 Hz will compensate for it and the overall HF band power has strongly correlated with that of the ECG.

III. Results

This section consists of four subsections. Section I discusses the proposed feature extraction techniques. Section II illustrates the ML classification results and, Section III illustrates the comparison of this work with the state of the art.

A. Proposed Feature Extraction Techniques

After acquiring and demodulating the radar data, we calculated the HRV time domain and frequency domain metrics from the observable events to use as features for machine learning classifiers. Following the analysis of patterns, we have categorized the features into two separate spaces (i.e., typical and hyper-features). Hyper-features are the dominant features, which show significant variation in different respiratory patterns. The extracted time domain and frequency domain HRV metrics have been enlisted in Table I according to their categories.

A single cycle of heartbeat includes two contractions, one is atrial contraction, and another is ventricular contraction [32]. Electrocardiogram (ECG) acquisition generally represents these contractions as a P wave for atrial contraction and a QRS complex waveform for ventricular contraction. R wave in the QRS wave complex is the maximum magnitude of a single heart cycle. Heartbeat signals are depicted by electric signals whereas the radar sensors capture the respiration patterns from the tiny movement of the chest surfaces that causes a phase change in the reflected signal [34], [35]. Unlike ECG signals, radar signals do not show discernible peaks for atrial or ventricular motions [36]. However, the highest peaks in radars correspond to R waves in ECG as illustrated in Fig. 3 and 4.

Hyper-feature Selection: The hyper-features were selected based on the significant variations of those features during

Authorized licensed use limited to: UNIV OF HAWAII LIBRARY. Downloaded on May 05,2025 at 21:27:57 UTC from IEEE Xplore. Restrictions apply.

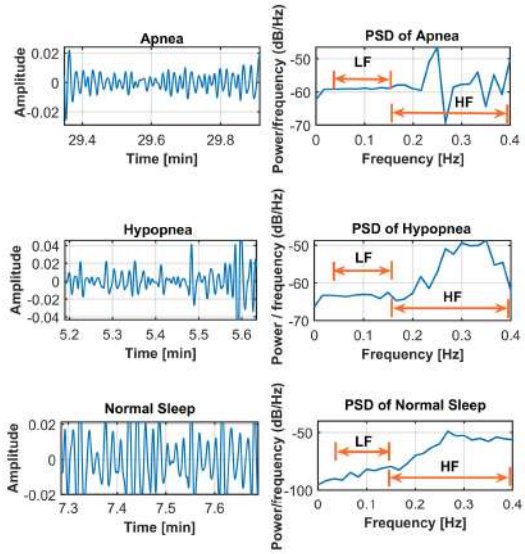

Fig. 5. Heart signals recorded during apnea, hypopnea and normal sleep (first column) and their respective PSDs (second column). The 0.04 to 0.15 Hz range in the PSDs are considered as low frequency band ranges whereas 0.15 to 0.4 Hz are high frequency band ranges. LF and HF are measured from the frequency components of low and high band ranges respectively.

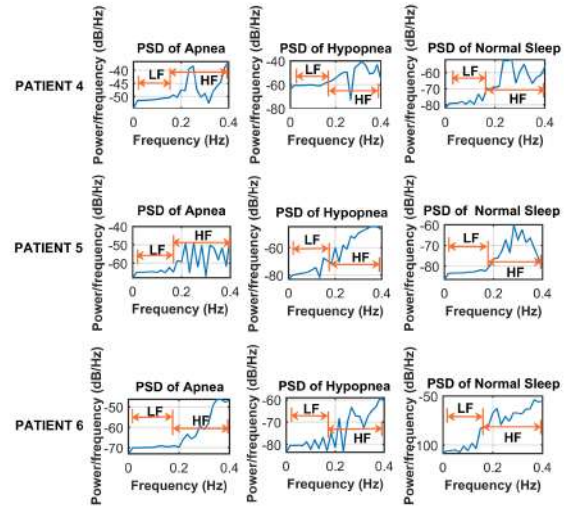

Fig. 6. PSDs of Apnea, Hypopnea and Normal breathing pattern during sleep of three different OSA patients. The HF power is significantly different for all the respiratory events and this variation can be seen for all the subjects as well. LF power of Apnea and Hypopnea events are higher compared to that of Normal events.

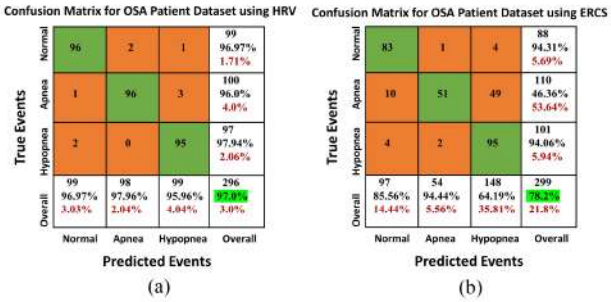

Fig. 7. Confusion matrix for OSA events classification showing the true and false-positive rates of the three events (Apnea, Hypopnea and Normal) using (a) HRV hyper-features LF and HF and (b) ERCS method. The overall classification accuracy for HRV and ERCS method are 97.0% and 78.2% respectively.

different respiratory events. In this investigation, we found LF and HF band powers as hyper-features as this particular feature changes significantly for different OSA events. HF power corresponds to the variation of HR in coordination with the respiration cycle [37], [38]. Heart rate increases during inhalation and decreases during exhalation [39]. Therefore, for different breathing patterns, the inhalation and exhalation periods are also different. This variation affects the HF band power. Consequently, for different OSA events, the HF band power has discernible values. The PSDs in Fig. 5 depict the variation of HF power for the different OSA events. We can also see the same variation for different subjects in Fig. 6. Hence, HF band power is referred to as a dominant feature. An increase in LF power is observed during slower breathing [39], [40]. Thus, apnea and hypopnea events will have a higher LF band power compared to normal events. The PSDs of Fig. 5 show the difference in the LF powers for different OSA events. The LF power of normal events can be seen as lower than that of apnea and hypopnea events. Different subjects exhibit the same variation in LF powers for different breathing patterns. The OSA events are perfectly distinguishable using LF and HF band powers, which is why they have been selected as hyper-features.

B. Machine Learning Classifiers

After extraction of HRV different features (normal and hyper-features) we used to train machine learning classifiers. 75% of the dataset was taken for training and 25% of the dataset was used for testing the ML classifiers. For the OSA clinical study dataset, we used 6 hours and 30 minutes of recorded clinical data from ten patients which contained 4728 breathing cycles (inhaling and exhaling), among them, the apnea cycle was almost1584 cycles, hypopnea 1560 cycles and normal breathing was 1584 cycles. For the classification of events from the HRV-based features, SVM, KNN, and Random Forest classifiers were used. The SVM classifier achieved the highest accuracy of 97.0% and outperformed the other classifiers. Fig. 7(a) illustrates the confusion matrix of the SVM model to classify the OSA events from the extracted HRV features. It is seen in the confusion matrix that 3% of apnea events were identified as hypopnea and 1% of data points were misclassified as normal events. Similarly, 2.06% of actual hypopnea events were classified as normal events. No hypopnea events were wrongly classified as apnea events. Moreover, 2.02% of normal events were predicted as apnea events and 1.01% as apnea events. Misclassification occurred mainly due to some hypopnea events having desaturation and arousal events mixed with them, which affects the HRV frequency metrics. Most of the sleep events were classified accurately with an overall accuracy of 97.0%. This underscores the efficacy of the proposed method. Table II illustrates the accuracy achieved by different ML classifiers for identifying different sleep events. In Table II, the accuracy for three different classifiers using the hyper-features and all the typical features

Authorized licensed use limited to: UNIV OF HAWAII LIBRARY. Downloaded on May 05,2025 at 21:27:57 UTC from IEEE Xplore. Restrictions apply.

TABLE II
ACCURACIES FOR DIFFERENT CLASSIFIERS

Classifiers	Accuracy	
	Hyper Feature	All Features
KNN	91.9%	86.8%
Random Forest	95.6%	93.9%
SVM	97%	94.9%

are shown. The results using only hyperfeatures outperform the results from all the features in each of the three models (KNN, SVM, Random Forest). This indicates the hyper-features LF and HF are unique and can clearly distinguish the events better than the typical features.

C. Comparison With HRV vs. Non-HRV Methods

Prior research on the classification of OSA events using Radar involved amplitude thresholding, machine learning on hand-crafted features, and deep learning [16], [20], [21]. Effective radar cross-section (ERCS) has been extracted from the five OSA patients to classify different events [20]. The ERCS method was implemented for a short-scale study with an accuracy of 96.7% [20]. Additionally, the reported results included only the analysis of selective 30 episodes of 60 seconds of each OSA event [20]. The IQ-imbalance and DC-offset estimation by employing center estimation algorithms is one of the difficulties with the ERCS technique using quadrature radar [39]. Numerous algorithms have been put forth, and it has been demonstrated that when the displacement length is tiny, the fitting error increases, and the center estimation algorithms are not given enough information [40]–[41]. Locating the circle to which the arc belongs and bringing its center to the origin of the complicated I-Q plot are the functions of the center estimation algorithm [20]. We also reanalyzed the ERCS method on the same clinical study dataset used here in this work. But, from Fig. 8 we can see that the arc received from the radar signals for the 2.4 GHz and 24 GHz radars for respiratory movement is lower than 40% of the total fitted circle which makes the imbalance correction erratic and challenging. As seen in Fig. 8, the arc radius for apnea, hypopnea, and normal events are close and due to wrong estimations, they can overlap easily. This results in misclassifications in differentiating apnea and hypopnea events. There were a total of 1196 sets of data of which 75% were taken for training and 25% for testing. The SVM classifier was used for the classification of OSA events. Fig. 6(b) illustrates the confusion matrix of the SVM model to classify the OSA events using the ERCS method. In another attempt [16], the signal amplitude thresholding technique was used to classify the OSA events. They validated their proposed method by comparing it with the results from the gold standard technique polysomnography (PSG) and achieved an accuracy of 75% in distinguishing apnea, hypopnea, and normal breathing patterns. A 2.4 GHz and 24 GHz radar is part of the PRMS monitoring system that was used to achieve high sensitivity

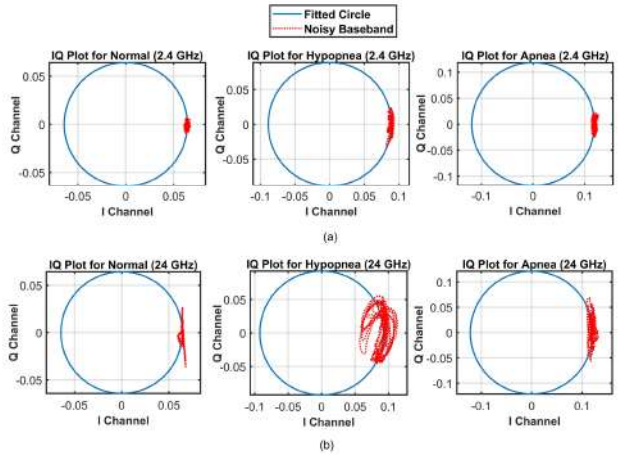

Fig. 8. Circle drawn from a radius of the arc of different OSA events (apnea, hypopnea, and normal) for (a) 2.4 GHz and (b) 24 GHz radar using the center estimation algorithm. The arcs of the 24 GHz radar are larger compared to the tiny arcs of the 2.4 GHz radar, which gives a better estimation of the center and a more accurate radius of the arc [39].

and high resolution. Previous results demonstrated the ability of 2.4 GHz to distinguish between normal and paradoxical breathing [16]. The resolution, however, is insufficient to discriminate between hypopnea and apnea. The 24 GHz radar, on the other hand, has difficulty identifying normal breathing while being successful in differentiating between apnea and hypopnea [16]. As a result, where paradoxical breathing was detected after evaluating both 2.4 GHz and 24 GHz, the 24 GHz result was used instead of the 2.4 GHz result. The success rate is increased. We also extracted HRV features from the 2.4 GHz and 24 GHz separately. In our investigation, we found that the LF and HF powers of the 24 GHz radar are 10 to 20 dB/Hz higher than the 2.4 GHz radar. For the 2.4 GHz radar, the LF power of apnea events ranges from −65 to −70 dB/Hz and HF power ranges from −40 to −60 dB/Hz. The LF and HF power of hypopnea events overlap with that of the apnea events for the 2.4 GHz radar, both having LF powers ranging from −65 to −70 dB/Hz and HF powers around −60 dB/Hz. This results in a smaller number of misclassifications between the apnea and hypopnea events, which is shown in Fig. 9(a). This overlap of apnea and hypopnea events doesn't occur for the 24 GHz radar. This leads to lesser misclassification and higher accuracy than the 2.4 GHz radar. For the 24 GHz radar, there are some overlaps between the LF and HF powers of hypopnea and normal breathing events. Both have LF powers in the −60 dB/Hz range and HF powers from −40 to −60 dB/Hz. This causes misclassification between hypopnea and normal events illustrated in the confusion matrix of Fig. 9(b). Combining the two radars lessens the overlap between the LF and HF powers and makes the apnea-hypopnea events more discernible. The accuracy of the combined frequency band dataset using the HRV method was around 97% and using the ERCS method the accuracy was around 78.2%. Our large-scale dataset analysis clearly illustrates that the accuracy of the HRV method superseded the non-HRV method (ERCS). A comparative analysis of this work with the state of the art has been shown in Table III.

Authorized licensed use limited to: UNIV OF HAWAII LIBRARY. Downloaded on May 05,2025 at 21:27:57 UTC from IEEE Xplore. Restrictions apply.

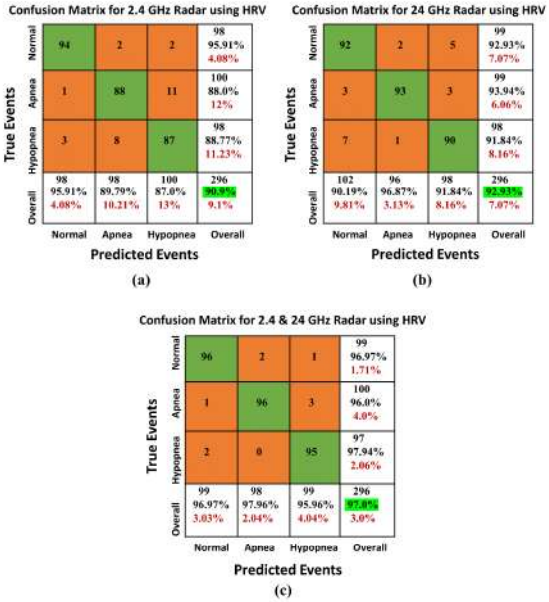

Fig. 9. Confusion matrix of OSA events classification showing the true and false-positive rates of the three events (apnea, hypopnea, and normal) for (a) 2.4 GHz radar, (b) 24 GHz radar, and (c) a mixture of 2.4 GHz & 24 GHz using the hyper-features LF and HF. The overall classification accuracy for the 2.4 GHz and 24 GHz radar were 90.9% and 92.93% respectively. When combined, the accuracy is 97%. These were calculated based on the average true-positive rate of the three events.

TABLE III
COMPARISON OF THIS PAPER WITH RECENT RELEVANT WORKS

Reference & year	Sensor	Feature Extraction	No. of Participants	Accuracy (%)
[21] 2022	60 GHz FMCW Radar	Convolutional Recurrent Neural Network (CRNN)	OSA Patient (44)	73.6%
[16] 2020	2.4 GHz & 24 GHz CW Radar	Amplitude thresholding using PRMS integrated into Sandman software	OSA Patient (10)	75%
[20] 2020	2.4 GHz CW Radar	Breathing rate from FFT and Square of Radius of Arc from ERCS using Quadratic SVM	OSA Patient (5) (Short Scale)	96.7%
			OSA Patient (10) (Large scale dataset)	78.2%
This work	2.4 GHz & 24 GHz CW Radar	HRV features (Time domain and frequency domain) using SVM classifier	OSA Patient (10)	97%

IV. CONCLUSION

This article proposes a robust HRV-based feature extraction technique to classify different respiratory events, such as apnea, hypopnea, and normal breathing patterns from the sleep study dataset of ten OSA patients. The authors also found hyper-features that are known as HF and LF show significant variations for different respiratory patterns. The extracted hyper-features were integrated with the traditional machine learning classifiers SVM, KNN, and Random Forest. The SVM classifier outperformed the other classifiers with an overall accuracy of 97% for the OSA patients dataset. The efficacy of the proposed robust method has been verified for the OSA patient's clinical study. The proposed HRV-based method has several potential applications including in-home respiratory disease diagnosis, health monitoring, and IoT applications.

ACKNOWLEDGMENT

The authors would like to thank their mentors Prof. Dr. Victor M. Lubecke and Prof. Dr. Olga Boric-Lubecke, University of Hawaii, USA for providing us with a clinical study dataset and the PI of this project has been working under the supervision of the mentors. OSA clinical study was approved by the Institutional Review Board protocol number 1484 of the University of Hawaii at Manoa. The sleep study used was approved by the Institutional Review Board of the University of Hawaii at Manoa (CHS#1484) and Queen's Medical Center (RA-2012-302). The sleep studies were carried out at a certified sleep study center at Queen's Medical Center (Honolulu, HI). 12 volunteers (2 for test and 10 for evaluation study) with known OSA were recruited for this study (mean age: 49 years, mean weight 215.2 $\pm$ 72.5 lbs, mean height 65.9 $\pm$ 4.5 inches, and mean BMI 35.1 $\pm$ 11.4) and provided with written consent prior to the study. The participants were not allowed to use a Continuous Positive Airway Pressure (CPAP) machine during the tests.

REFERENCES

[1] National Research Council, *Sleep Disorders and Sleep Deprivation: An Unmet Public Health Problem*. Washington, DC, USA: National Academic Press, 2006. [Online]. Available: http://iom.edu/Reports/2006/Sleep-Disorders-and-Sleep-Deprovation-an-unment-public-health-problem.aspx

[2] V. K. Somers et al., "Sleep apnea and cardiovascular disease," *J. Amer. College Cardiol.*, vol. 52, pp. 686–717, Aug. 2008.

[3] S. M. Caples, A. S. Gami, and V. K. Somers, "Obstructive sleep apnea," *Ann. Intern. Med.*, vol. 142, pp. 187–197, Feb. 2005.

[4] J.-D. Lattimore, D. S. Celermajer, and I. Wilcom, "Obstructive sleep apnea and cardiovascular disease," *J. Amer. College Cardiol.*, vol. 41, pp. 1429–1437, May 2003.

[5] E. J. Olson, W. R. Moore, T. I. Morgenthaler, P. C. Gay, and B. A. Staats, "Obstructive sleep apnea-hypopnea syndrome," *Mayo Clin. Proc.*, vol. 78, no. 12, pp. 1545–1552, Dec. 2003.

[6] D. A. Pevernagie et al., "On the rise and fall of the apnea−hypopnea index: A historical review and critical appraisal," *J. Sleep Res.*, vol. 29, no. 4, Aug. 2020, Art. no. e13066, doi: 10.1111/jsr.13066.

[7] V. K. Kapur et al., "Clinical practice guideline for diagnostic testing for adult obstructive sleep apnea: An American academy of sleep medicine clinical practice guideline," *J. Clin. Sleep Med.*, vol. 13, no. 03, pp. 479–504, Mar. 2017, doi: 10.5664/jcsm.6506.

[8] P. J. Strollo and R. M. Rogers, "Obstructive sleep apnea," *New England J. Med.*, vol. 334, no. 2, pp. 99–104, 1996.

[9] G. Matar, J.-M. Lina, J. Carrier, and G. Kaddoum, "Unobtrusive sleep monitoring using cardiac, breathing and movements activities: An exhaustive review," *IEEE Access*, vol. 6, pp. 45129–45152, 2018, doi: 10.1109/ACCESS.2018.2865487.

[10] M. De Zambotti, N. Cellini, A. Goldstone, I. M. Colrain, and F. C. Baker, "Wearable sleep technology in clinical and research settings," *Med. Sci. Sports Exercise*, vol. 51, no. 7, pp. 1538–1557, Jul. 2019, doi: 10.1249/MSS.0000000000001947.

[11] V. P. Tran, A. A. Al-Jumaily, and S. M. S. Islam, "Doppler radar-based non-contact health monitoring for obstructive sleep apnea diagnosis: A comprehensive review," *Big Data Cogn. Comput.*, vol. 3, no. 1, Jan. 2019, Art. no. 3, doi: 10.3390/bdcc3010003.

[12] A. P. Addison, P. S. Addison, P. Smit, D. Jacquel, and U. R. Borg, "Non-contact respiratory monitoring using depth-sensing cameras: A review of current literature," *Sensors*, vol. 21, no. 4, Feb. 2021, Art. no. 1135, doi: 10.3390/s21041135.

[13] S. M. M. Islam, "Radar-based remote physiological sensing: Progress, challenges, and opportunities," *Front. Physiol.*, vol. 13, Oct. 2022, Art. no. 955208, doi: 10.3389/fphys.2022.955208.

Authorized licensed use limited to: UNIV OF HAWAII LIBRARY. Downloaded on May 05,2025 at 21:27:57 UTC from IEEE Xplore. Restrictions apply.

[14] S. M. M. Islam, O. Boric-Lubecke, V. M. Lubecke, A.-K. Moadi, and A. E. Fathy, "Contactless radar-based sensors: Recent advances in vital-signs monitoring of multiple subjects," *IEEE Microw. Mag.*, vol. 23, no. 7, pp. 47–60, Jul. 2022, doi: 10.1109/MMM.2022.3140849.

[15] Y. Zhou et al., "Validation of novel automatic ultra-wideband radar for sleep apnea detection," *J. Thoracic Dis.*, vol. 12, no. 4, pp. 1286–1295, Apr. 2020, doi: 10.21037/jtd.2020.02.59.

[16] M. Baboli, A. Singh, B. Soll, O. Boric-Lubecke, and V. M. Lubecke, "Wireless sleep apnea detection using continuous wave quadrature Doppler radar," *IEEE Sensors J.*, vol. 20, no. 1, pp. 538–545, Jan. 2020, doi: 10.1109/JSEN.2019.2941198.

[17] A. Q. Javaid, C. M. Noble, R. Rosenberg, and M. A. Weitnauer, "Towards sleep apnea screening with an under-the-mattress IR-UWB radar using machine learning," in *Proc. IEEE 14th Int. Conf. Mach. Learn. Appl.*, 2015, pp. 837–842, doi: 10.1109/ICMLA.2015.79.

[18] H. Zhao et al., "A noncontact breathing disorder recognition system using 2.4-GHz digital-IF Doppler radar," *IEEE J. Biomed. Health Inform.*, vol. 23, no. 1, pp. 208–217, Jan. 2019, doi: 10.1109/JBHI.2018.2817258.

[19] S. Kang et al., "Non-contact diagnosis of obstructive sleep apnea using impulse-radio ultra-wideband radar," *Sci. Rep.*, vol. 10, no. 1, Dec. 2020, Art. no. 5261, doi: 10.1038/s41598-020-62061-4.

[20] F. Snigdha, S. M. M. Islam, O. Boric-Lubecke, and V. Lubecke, "Obstructive sleep apnea (OSA) events classification by effective radar cross section (ERCS) method using microwave Doppler radar and machine learning classifier," in *Proc. IEEE Microw. Theory Technol. Soc. Int. Microw. Biomed. Conf.*, 2020, pp. 1–3.

[21] J. W. Choi et al., "Automated detection of sleep apnea-hypopnea events based on 60 GHz frequency-modulated continuous-wave radar using convolutional recurrent neural networks: A preliminary report of a prospective cohort study," *Sensors*, vol. 22, no. 19, Sep. 2022, Art. no. 7177, doi: 10.3390/s22197177.

[22] S. M. M. Islam and V. M. Lubecke, "Sleep posture recognition with a dual-frequency microwave Doppler radar and machine learning classifiers," *IEEE Sens. Lett.*, vol. 6, no. 3, Mar. 2022, Art. no. 3500404, doi: 10.1109/LSENS.2022.3148378.

[23] V. C. C. Sequeira, P. M. Bandeira, and J. C. M. Azevedo, "Heart rate variability in adults with obstructive sleep apnea: A systematic review," *Sleep Sci.*, vol. 12, no. 3, 2019, Art. no. 214, doi: 10.5935/1984-0063.20190082.

[24] Z. Wang et al., "Heart rate variability changes in patients with obstructive sleep apnea: A systematic review and meta-analysis," *J. Sleep Res.*, vol. 32, no. 1, 2023, Art. no. e13708, doi: 10.1111/jsr.13708.

[25] S. Hietakoste et al., "Longer apneas and hypopneas are associated with greater ultra-short-term HRV in obstructive sleep apnea," *Sci. Rep.*, vol. 10, 2020, Art. no. 21556, doi: 10.1038/s41598-020-77780-x.

[26] "K-MC1 Radar transceiver," May 10, 2010. [Online]. Available: https://www.rfbeam.ch/product/k-mc1-radar-transceiver/

[27] M. S. Ishrak, F. Cai, S. M. M. Islam, O. Borić-Lubecke, T. Wu, and V. M. Lubecke, "Doppler radar remote sensing of respiratory function," *Front. Physiol.*, vol. 14, Apr. 2023, Art. no. 1130478, doi: 10.3389/fphys.2023.1130478.

[28] B.-K. Park, S. Yamada, O. Boric-Lubecke, and V. Lubecke, "Single-channel receiver limitations in Doppler radar measurements of periodic motion," in *Proc. IEEE Radio Wireless Symp.*, 2006, pp. 99–102, doi: 10.1109/RWS.2006.1615104.

[29] B.-K. Park, O. Boric-Lubecke, and V. M. Lubecke, "Arctangent demodulation with DC offset compensation in quadrature Doppler radar receiver systems," *IEEE Trans. Microw. Theory Techn.*, vol. 55, no. 5, pp. 1073–1079, May 2007, doi: 10.1109/TMTT.2007.895653.

[30] F. Shaffer, R. McCraty, and C. L. Zerr, "A healthy heart is not a metronome: An integrative review of the heart's anatomy and heart rate variability," *Front. Psychol.*, vol. 5, 2014, Art. no. 1040, doi: 10.3389/fpsyg.2014.01040.

[31] H. Wu, X. Zhan, M. Zhao, and Y. Wei, "Mean apnea-hypopnea duration (but not apnea-hypopnea index) is associated with worse hypertension in patients with obstructive sleep apnea. Medicine (Baltimore)," *Medicine*, vol. 95, no. 48, Nov. 2016, Art. no. e5493, doi: 10.1097/MD.0000000000005493.

[32] F. Shaffer and J. P. Ginsberg, "An overview of heart rate variability metrics and norms," *Front. Public Health*, vol. 5, 2017, Art. no. 258, doi: 10.3389/fpubh.2017.00258.

[33] M. S. Hossain, S. D. Uddin, and S. M. M. Islam, "Heart rate variability assessment using single channel CW Doppler radar," in *Proc. IEEE Microw. Theory Technol. Soc. Antennas Propag. Soc. Microw., Antennas, Propag.*, 2023, pp. 325–330.

[34] N. H. M. Sani, W. Mansor, K. Y. Lee, N. A. Zainudin, and S. A. Mahrim, "Determination of heart rate from photoplethysmogram using fast Fourier transform," in *Proc. Int. Conf. BioSignal Anal., Process. Syst.*, 2015, pp. 168–170, doi: 10.1109/ICBAPS.2015.7292239.

[35] S. Andreas, G. Hajak, B. von Breska, E. Rüther, and H. Kreuzer, "Changes in heart rate during obstructive sleep apnoea," *Eur. Respir. J.*, vol. 5, no. 7, pp. 853–857, Jul. 1992.

[36] S. S. Mader and M. Windelspecht, "Human biology," McGraw Hill, p. 21, Jan. 1, 2012.

[37] O. Boric-Lubecke, V. M. Lubecke, A. D. Droitcour, B.-K. Park, and A. Singh, "Doppler radar physiological sensing," Dec. 30, 2015. Accessed: Sep. 30, 2022. [Online]. Available: https://www.wiley.com/en-us/Doppler+Radar+Physiological+Sensing-p-9781118024027

[38] J.-Y. Kim, J.-H. Park, S.-Y. Jang, and J.-R. Yang, "Peak detection algorithm for vital sign detection using Doppler radar sensors," *Sensors*, vol. 19, no. 7, Apr. 2019, Art. no. 1575, doi: 10.3390/s19071575.

[39] P. Grossman and E. W. Taylor, "Toward understanding respiratory sinus arrhythmia: Relations to cardiac vagal tone, evolution and biobehavioral functions," *Biol. Psychol.*, vol. 74, no. 2, pp. 263–285, Feb. 2007, doi: 10.1016/J.BIOPSYCHO.2005.11.014.

[40] D. L. Eckberg and M. J. Eckberg, "Human sinus node responses to repetitive, ramped carotid baroreceptor stimuli," *Amer. J. Physiol.*, vol. 242, no. 4, pp. H638–H644, 1982, doi: 10.1152/AJPHEART.1982.242.4.H638.

[41] D. K. Kim and Y. Kim, "Quadrature frequency-group radar and its center estimation algorithms for small vibrational displacement," *Sci. Rep.*, vol. 9, no. 1, May 2019, Art. no. 6763, doi: 10.1038/s41598-019-43205-7.

Syed Doha Uddin (Student Member, IEEE) received the B.Sc. degree in electrical and electronic engineering from the University of Dhaka, Dhaka, Bangladesh, in 2023. He is currently working toward the Ph.D. degree in electrical engineering from Texas Tech University, Lubbock, TX, USA. His research interests include radar signal processing, vital signs monitoring, and non-contact sensing.

Md. Shafkat Hossain (Student Member, IEEE) received the B.Sc. degree in electrical and electronic engineering, in 2023 from the University of Dhaka, Dhaka, Bangladesh, where he is currently working toward the M.Sc. degree in electrical and electronic engineering. He is currently the Vice-Chair of the IEEE Microwave Theory and Technology Society Student Branch Chapter, University of Dhaka. His research interests include radar signal processing, radar based vital signs monitoring, and remote sensing.

Shekh M. M. Islam (Senior Member, IEEE) received the B.Sc. (Hons.) and M.Sc. degrees in electrical and electronic engineering from the University of Dhaka, Dhaka, Bangladesh, in 2012 and 2014, respectively, and the Ph.D. degree in electrical engineering from the University of Hawaii at Manoa, Honolulu, HI, USA, with a focus on biomedical applications incorporating RF/Microwave technologies in 2020. He is currently an Assistant Professor with the Department of Electrical and Electronic Engineering, University of Dhaka. He is also a JSPS Invitational Fellow with Kyoto University, Kyoto, Japan. His research interests include radar systems, antenna array signal processing, adaptive filter techniques, and machine-learning classifiers for pattern recognition. In the Summer of 2019, he was also a Radar System and Applications Engineering Intern with ON Semiconductor, Phoenix, AZ, USA. He has also been an Affiliate Member of the technical committee of the MTT-28 Biological Effects and Medical Applications of the IEEE Microwave Theory and Technique Society. He was the recipient of the 2020 University of Hawaii at Manoa Department of Electrical Engineering Research Excellence Award. He was also the student paper finalist at the IEEE Radio Wireless Week (RWW'19) conference, which was held in FL, USA. He has also been an Editorial Board Member of Frontiers in Physiology journal and a Review Editor of IEEE ACCESS, IEEE SENSORS, IEEE TRANSACTIONS ON MICROWAVE THEORY AND TECHNIQUES, and IEEE JOURNAL OF ELECTROMAGNETICS, RF AND MICROWAVES.

Victor Lubecke, photograph and biography not available at the time of publication.

Authorized licensed use limited to: UNIV OF HAWAII LIBRARY. Downloaded on May 05,2025 at 21:27:57 UTC from IEEE Xplore. Restrictions apply.